arXiv:1602.03282v2 [cond-mat.other] 25 Aug 2016

Superfluid behavior of quasi-1D p-H_2 inside carbon nanotube

Maurizio Rossi[1,2] and Francesco Ancilotto[3,4]

[1]*Scuola Normale Superiore, Piazza dei Cavalieri 7, I-56126 Pisa, Italy*
[2]*International Center for Theoretical Physics (ICTP), Strada Costiera 11, I-34154 Trieste, Italy*
[3]*Dipartimento di Fisica e Astronomia "Galileo Galilei" and CNISM, Università di Padova, via Marzolo 8, 35122 Padova, Italy*
[4]*CNR-IOM Democritos, via Bonomea, 265 - 34136 Trieste, Italy*

(Dated: August 26, 2016)

We perform ab-initio Quantum Monte Carlo simulations of para-hydrogen (pH_2) at $T = 0$ K confined in carbon nanotubes (CNT) of different radii. The radial density profiles show a strong layering of the pH_2 molecules which grow, with increasing number of molecules, in solid concentric cylindrical shells and eventually a central column. The central column can be considered an effective one-dimensional (1D) fluid whose properties are well captured by the Tomonaga-Luttinger liquid theory. The Luttinger parameter is explicitly computed and interestingly it shows a non-monotonic behavior with the linear density similar to what found for pure 1D ^{3}He. Remarkably, for the central column in a (10,10) CNT, we found an ample linear density range in which the Luttinger liquid is (i) superfluid and (ii) stable against a weak disordered external potential, as the one expected inside realistic pores. This superfluid behavior could be experimentally revealed in bundles of carbon nanotubes, where deviations from classical inertial values associated with superfluid density could be measured by using quartz crystal microbalance techniques. In summary, our results suggest that pH_2 within carbon nanopores could be a practical and stable realization of the long sought-after, elusive superfluid phase of parahydrogen.

PACS numbers: 67.25.D-, 67.25.dr

Superfluid para-hydrogen (pH_2) represents one of the most elusive phases in Nature. As liquid helium, pH_2 is a natural candidate for displaying superfluidity by virtue of its light mass. Contrarily to helium however, it does not remains liquid down to zero temperature as a consequence of the stronger attractive interaction, which is about four times larger than the He-He one, and undergoes a crystallization transition around 14 K [1] (at saturated vapor pressure), a temperature much higher than the calculated superfluid bulk transition temperature $T \sim 1.1\,K$ [2]. To create superfluid pH_2 it is therefore necessary to bring the liquid below its saturated vapor pressure curve. Attempts to produce a bulk superfluid pH_2 sample by supercooling the normal liquid below the triple point have been unsuccessful so far [3].

As a possible way to stabilize the liquid phase of pH_2 at low temperatures several authors have considered restricted geometries to reduce the effective attraction between molecules, and thus the zero-pressure density. For example, the lowering of the melting point compared to the bulk liquid is a well-known and rather general phenomenon in clusters [4], and a widely explored route in the search for pH_2 superfluidity is indeed based upon the realization and study of ultra-small pH_2 clusters. The associated reduction of scale suggests that pH_2 clusters could display superfluidity. This expectation is based on the fact that the smaller number of neighbors and surface effects in small clusters may hinder solidification and promote a liquid-like phase at low temperature[5]. The first prediction of superfluidity in pH_2 clusters made of few molecules was reported in 1991 based on quantum Monte Carlo (QMC) simulations [6]. The first experimental signature of superfluidity in pH_2 was in fact inferred from the un-hindered rotation of a chromophore molecule in a cluster made of $N = 15$ pH_2 molecules embedded in a larger ^{4}He nanodroplet [7]. Even if larger droplets of pH_2 are found to remain liquid at low temperature [5], experiments of non-classical rotation seem to locate the maximum size for a superfluid cluster at $N = 17$ [8]. Despite the great effort devoted to such systems [9], any attempt of a direct observation of a stable superfluid phase of pH_2 has so far failed.

Another possibility put forward in theoretical calculations is to exploit disorder for suppressing crystallization and promote a superfluid response. However, even in the most favorable scenario, disorder gives rise to a glassy phase which is predicted to be superfluid in a metastable regime [10] but not at equilibrium [11].

Taking advantage of the understanding gained for ^{4}He systems, geometrical confinement has been considered too as a possible route to stabilize a bulk superfluid phase for pH_2. In fact, as inferred from extensive investigations for ^{4}He in porous media such as Vycor [12], zeolites [13], and aerogel [14], as well as in superfluid films [15], quantum fluids in constrained geometries behaves differently than in the bulk. Equivalent indications of possible superfluid behavior for pH_2 in nanoconfined systems are scarce and often contradictory. A possible superfluid phase inside a (5,5) carbon nanotube was predicted by studying the equation of state of pure one dimensional (1D) pH_2 at $T = 0$ K with Diffusion Monte Carlo [16]. However, recent Path Integral Monte Carlo (PIMC) cal-

culations seem to contradict this claim, by showing that the 1D pH_2 equilibrium phase is a crystal [17], as it also is in 2D pH_2 [18].

So far the only reported enhancement of superfluid response was obtained within PIMC simulations for pH_2 confined inside nano-cavities [19]. The confining medium discussed in this paper is however not realistic, being composed of spherical nano-sized cavities coated with alkali metal thick films in order to reduce the adsorption properties of the cavity walls, which seems hardly feasible at the present time.

We follow here a different approach by addressing a more realistic system made of pH_2 molecules in a confining system that is routinely provided by existing nanotechnologies, i.e. armchair carbon nanotubes (CNT) of different radii. Although strictly 1D geometry precludes superfluid behavior, wider tubes where pH_2 forms a quasi-1D system coexisting with solid-like concentric cylindrical shells could provide the ideal environment where strong evidence of the elusive superfluidity of parahydrogen could be collected, as shown in the present work.

Our calculations are based on exact zero temperature Path Integral Ground State (PIGS) Monte Carlo method [20, 21]. Because PIGS is a well-established computational methodology we shall not review it here. We recall only that the most relevant feature is that it provides unbiased estimates of the $T = 0$ K ground state properties directly by the microscopic Hamiltonian, by projecting in imaginary time a trial wave function. The quality of the trial wave function has the sole role to fix the length of the total imaginary time projection. Here we have considered a shadow wave function (SWF) [22], which has provided an optimal trial wave function for bulk [23], confined [24], overpressurized [25] and dimensionally reduced [26] ^{4}He systems, whose parameters have been optimized to describe pH_2 [27]. All the approximations involved in the PIGS method, i.e. the choice of the total imaginary time τ, of the imaginary time step $\delta\tau$ and the approximation for the short imaginary time propagator, are so well controlled that the resulting systematic errors can be reduced within the unavoidable Monte Carlo statistical error making of PIGS an *exact* zero-temperature method [20, 21].

In our calculations we consider N pH_2 molecules, described as point-like particle with zero spin adsorbed within CNT of different radii, described by the following Hamiltonian

$$\hat{H} = -\lambda \sum_i \nabla_i^2 + \sum_{i<j} v(|\vec{r}_i - \vec{r}_j|) + \sum_i V(\vec{r}_i), \qquad (1)$$

where $\vec{r}_i$ are the positions of the pH_2 molecules, $\lambda = \hbar^2/2m = 12.031$ KÅ^2, v describes the interaction between a pair of molecules and V describes the interaction of a molecule with the CNT. We assume periodic boundary conditions along the tube axis. As for v, which is considered spherically symmetric, we use the well-known Silvera-Goldman potential (SG) [28]. We specifically consider three different armchair CNTs: the $(10, 10)$ CNT with radius $R = 6.80$ Å, the $(12, 12)$ CNT with radius $R = 8.19$ Å and the $(15, 15)$ CNT with radius $R = 10.17$ Å. To model the H_2-carbon interaction we used a pair potential fitted to high level ab initio results on the interaction between H_2 and graphite [1]. This procedure provides a corrugated potential V, but implicitly neglects the effects of curvature, which however are found to have very little consequences for the considered CNTs [30]. By using the fourth order pair-Suzuki approximation [21] for the short imaginary time propagator we observe convergence of ground state estimates with a projection time $\tau = 0.250$ K^{-1} using a time step $\delta\tau = 1/640$ K^{-1}.

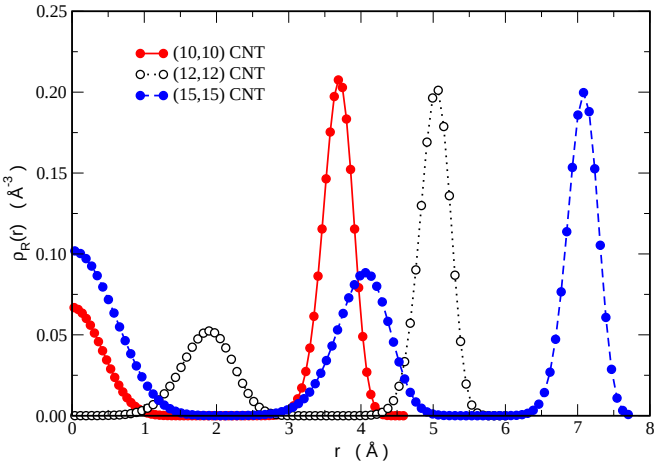

FIG. 1: (Color online) Typical radial density profiles $\rho_R(r)$ for pH_2 inside the considered CNTs. Statistical errors are smaller than the used symbols.

We made a number of simulations with varying number N of pH_2 molecules from 38 up to a maximum of 432, adsorbed within the three different CNTs of increasing length $14.77 < L < 59.00$ Å. Similarly to the case of ^{4}He adsorbed in nanotubes [31–36], the pH_2 radial density profiles $\rho_R(r)$, reported in Fig. 1, show a marked layered structure: the pH_2 molecules form a cylindrical shell adsorbed on the inner tube wall plus a central column in the (10,10) CNT, two concentric cylindrical shells in the (12,12) CNT, and two concentric cylindrical shells plus a central column in the (15,15) CNT. The promotion to the second (lower density) layer (or to the central column for the (10,10) CNT) occurs at an areal density value $\theta_P = 0.108$ Å^{-2}, which is about 15% higher than the promotion coverage to the second layer found for pH_2 adsorbed on graphite [37]. For all the three CNT, the adsorbed layer adjacent to the tube inner surface turns out to be a crystalline two dimensional triangular solid wrapped to form a cylinder, whose structure is incommensurate with the underlying carbon lattice. The intermediate shells (in the (12,12) and (15,15) tubes) are

also two dimensional solid wrapped on a cylindrical surface for all the considered values of N, with no evidence whatsoever of a liquid-like behavior.

Within the PIGS method it is possible to obtain a direct estimate of the superfluid fraction ρ_s from the imaginary time diffusion of the center of mass of the system [38, 39]. For the (10,10) and (12,12) CNTs, we found a sizable superfluid response, comparable with the (debated [40]) one calculated for pH_2 embedded in a 2D Na crystal [41]. However, this large ρ_s has to be ascribed to the presence of defects in the crystalline structure of the adsorbed layer due to the mismatch between the pH_2 lattice and the underlying carbon structure, i.e. to the actual length L of the simulated CNT. The effective ability of such defects to sustain a detectable superfluid flow [42] or rather their pinning at the structural defects in real CNTs is beyond the scope of this paper.

Our systems provide however a better candidate for superfluidity: the central column in (10,10) and (15,15) CNTs, that behaves as a quasi-1D superfluid whose properties are well captured by the Tomonaga-Luttinger liquid theory (TLL) [43–45]. The description of a confined quantum fluid by means of the TLL has been successfully applied to ^{4}He in nanopores [33, 34].

TLL is a phenomenological theory than captures the low-energy properties of a wide class quantum 1D systems with short range interaction [43, 46] in terms of two bosonic fields, $\phi(x)$ and $\theta(x)$ representing respectively the density and the phase fluctuations of the particle field operator $\psi(x) = \sqrt{\rho + \partial_x \phi(x)}\, e^{i\theta(x)}$ (ρ being the average density) via the low-energy effective Hamiltonian

$$H_{LL} = \frac{\hbar}{2\pi} \int dx \left(c K_L \partial_x \theta(x)^2 + \frac{c}{K_L} \partial_x \phi(x)^2 \right) \quad . \quad (2)$$

The parameter K_L (known as Luttinger parameter [47]) and the velocity c are generally independent quantities fixed by the microscopic details of the system. Such Hamiltonian is exactly solvable, thus the knowledge of c and K_L is enough to characterize the correlation functions and the thermodynamic properties of the system. For Galilean-invariant systems, as the ones we are going to consider here, $c = \hbar\pi\rho/mK_L$ [45], thus the only parameter to be determined is K_L. Here we determine the Luttinger paramenter via QMC simulations, that have largely been proven to ba efficient in estimating K_L [17, 48–50].

K_L governs the decay of correlations function and can be used to draw a well defined definition of (quasi) crystal and (quasi) superfluid. For $K_L < 1/2$ the static structure factor develops Bragg peaks at reciprocal lattice vectors, which is the signature of a (quasi) crystalline solid. For $K_L > 1/2$ no (quasi) diagonal-long range order is present, but the system displays a (quasi) off-diagonal long-range order. Thus, even if no true long-range order can exist in 1D for a system of particles with short range interaction [51], there can be a phase, known as Luttinger liquid (LL), featuring power-law decaying correlations [45], that is superfluid in the sense that it displays a quasi-off diagonal long range order [52, 53]. Such a superfluidity manifests different degree of robustness against disorder or external potentials. Specifically, if $K_L > 3/2$ the superfluid is insensitive to a weak external disordered potential [54], while for a periodic external potential commensurate with the density with filling fraction $1/p$, the transition is located at $K_L = 2/p^2$ [53].

It was found that for narrow pores ^{4}He obeys the TLL theory with a small Luttinger parameter corresponding to solid-like character of the adsorbed phase [33, 34]. On the other hand, for wider pores, the central region appears to behave like a LL but with a larger K_L indicating that the system is dominated by superfluid fluctuations, as indeed expected for superfluid ^{4}He. We will show here that a similar behavior occurs for pH_2 in CNTs. Since the exchanges of molecules with the surrounding shells are null, the central column of pH_2 in (10,10) and (15,15) CNT can be considered an effective one-dimensional system that can be well described via the TLL [34]. The surrounding shells have the crucial role to screen (reduce) the bare pH_2-pH_2 interaction, and the molecules inside the central column can be depicted as pure 1D particles (with the same mass of the initial ones) interacting via the effective potential [34]

$$v_{1D}(z) = \frac{1}{\rho_L^2} \int d^2r \int d^2r' v(\vec{r} - \vec{r}') \rho_R(r) \rho_R(r') \quad (3)$$

where $\vec{r} = (r, \varphi, z)$ is a vector in cylindrical coordinates and

$$\rho_L = \frac{N}{L} = 2\pi \int dr\ r \rho_R(r) \quad (4)$$

is the linear density. The resulting effective potential is almost insensitive to the actual pore length and to the density of the central column itself. The obtained v_1 for the (10,10) and (15,15) CNT are shown in Fig. 2, where they are also compared to the SG pH_2-pH_2 bare interaction potential. Notably, they can be fairly fitted by using a Lennard-Jones like formula [55]. As already observed for ^{4}He [34], the effect of the surrounding shells is that of reducing the potential well depth and of shifting the minimum to smaller separations. This can change dramatically the low-density behavior of the effective 1D system when compared to the strictly 1D pH_2. In fact, for example, pure 1D pH_2 is expected to display a spinodal decomposition at densities below 0.209 Å^{-1} [17], while we have been able to simulate such effective pure 1D system down to $\rho = 0.02$ Å^{-1} without any signature of spinodal decomposition. For this pure 1D system, we have simulated $N = 50$ particles in order to minimize the finite size effects [17, 50], taking $\tau = 2.50$ K^{-1} and $\delta\tau = 1/320$ K^{-1} to guarantee convergence to the ground state.

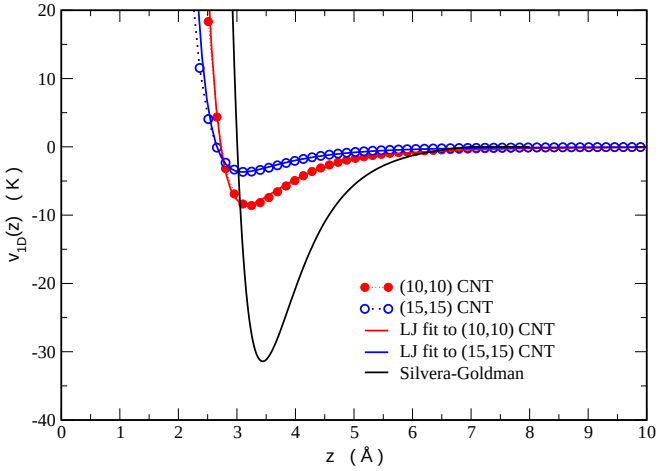

FIG. 2: (Color online) Effective one-dimensional interaction potential v_{1D}, obtained by Eq. (3), for pH_2 molecules in the central column inside (10,10) and (15,15) CNT. The effective potentials are compared with the Silvera-Goldman potential for the pH_2-pH_2 interaction. Continuous lines represent a fit of v_{1D} with a Lennard-Jones (LJ) like potential.

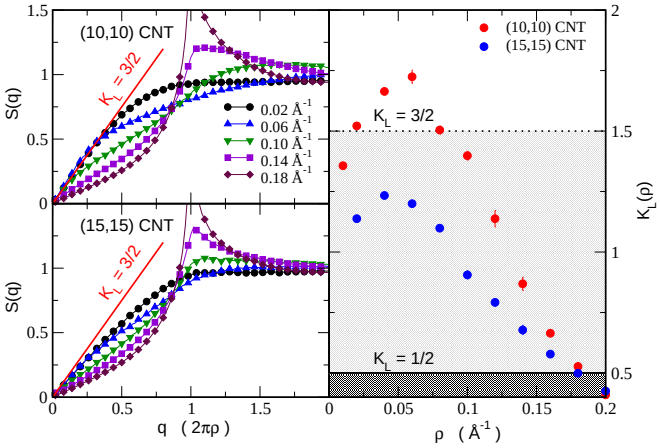

FIG. 3: (Color online) Left: static structure factors S(q) for both the effective 1D systems realized by the central column of pH_2 inside the (10,10) and the (15,15) CNT for different linear densities ρ. The momenta q are given in units of $2\pi\rho$. Errorbars are smaller than the used symbols. The straight red line marks the threshold $K_L = 3/2$. Right: Luttinger parameter K_L as obtained by the low momenta behavior of the static structure factor. Both the relevant thresholds $K_L = 1/2$ (which discerns from a (quasi) crystal and a (quasi) superfluid) and $K_L = 3/2$ (which marks the stability of the superfluid against a weak disordered external potential) are also shown.

The Luttinger parameter K_L can be extracted by the low momenta behavior of the static structure factor $S(k)$ [49, 50]

$$S(k) = \frac{K_L k}{2\pi\rho}, \qquad k \to 0. \tag{5}$$

Some example of the calculated $S(k)$ for the effective 1D systems realized by the central column of pH_2 inside the (10,10) and the (15,15) CNT are reported in Fig. 3 for different values of the linear density ρ. The linear behavior at low momenta is evident and the extracted K_L are reported in the right panel of the same figure. The dependence of K_L from the density is non-monotonic and resembles the one for ^{3}He [49].

The key result of the present work is however that for the central column of pH_2 inside a (10,10) CNT there is an ample density range ($0.02 < \rho < 0.08$ Å^{-1}) where $K_L > 3/2$, meaning that the LL is both superfluid and stable against the presence of a weak disordered external potential. The stability of such a 1D superfluid is crucial because pH_2 inside the central column is expected to indeed experience an external potential. For the (10,10) CNT, the potential provided by the CNT itself is practically flat on the pore axis, while the one provided by the surrounding solid layer is weak and disordered because of incommensurability effects [56]. No stable LL superfluid has been observed for the (15,15) CNT, where the K_L is always lower than 3/2. It is interesting to note that the central columns in both the CNT undergo a crystal-superfluid transition at linear densities closed to the spinodal decomposition of the pure pH_2.

A possible way to experimentally stabilize the superfluid phase of pH_2 is by confining it within aligned bundles of micron-sized parallel CNTs. The predicted superfluid phase of pH2 could be observed by using current quartz microbalance techniques [30], by measuring the frequency shifts in the shear modes of the microbalance parallel to the bundle axis. The density range where a superfluid response should be expected could be easily reached by changing the pressure (chemical potential) of the pH_2 vapor surrounding the nanotube bundles, which determines the actual amount of fluid adsorbed inside the central columns.

While preparing this manuscript, we were made aware of a recent paper where quasi-1D pH_2 in model nanopores with smooth walls was studied by using PIMC [57] with no sign of any LL-superfluid phase. When their radius is such that the pore houses a single pH_2 column, K_L is found to grows from the value 0.28 of the pure 1D pH_2 [17] to values close to 1/2 but still in the (quasi) crystalline state. Even the combination of cylindrical shell plus central column has been explored in Ref. [57] for a glass pore of radius $R = 5$ Å, but with opposite results than ours. We argue that the less attractive substrate and the small radius with respect to the (10,10) CNT considered here, provide a tighter confinement for pH_2 that strongly localizes the molecules, resulting in a Luttinger parameter even lower than the one of the pure pH_2.

In conclusion we have studied, by using PIGS exact simulations and the TLL theory, pH_2 within geometric confinement provided by realistic CNT of different radii. The results show the appearance, for the (10,10)

and (15,15) CNTs, of a central column along the NT axis, that can be described within the TLL theory. The molecules belonging to the inner column are screened by the solid pH_2 layers adsorbed on the surrounding CNT inner wall, resulting in pronounced quantum exchanges between molecules within the column, leading to a clear superfluid behavior in the (10,10) CNT. Our QMC simulations do indeed confirm this scenario, suggesting that pH_2 within bundles of carbon nanotubes could be a practical realization of the elusive superfluid phase of parahydrogen.

We thank M. Boninsegni, G. Bertaina, D.E. Galli, G. Mistura and P.L. Silvestrelli for stimulating discussions.

[1] A.C. Clark, X. Lin and M.H.W. Chan, Phys. Rev. Lett. **97**, 245301 (2006).

[2] S.M.Apenko, Phys. Rev. B **60**, 3052 (1999); V.S. Vorob'ev and S.P. Malyshenko, J. Phys. Cond. Matter **12**, 5071 (2000

[3] H.J. Maris, G.M. Seidel and T.E. Huber, J. Low Temp. Phys. **51**, 471 (1983).

[4] J.A. Alonso, *Structure and Properties of Atomic Clusters*. (Imperial College Press, London, 2005).

[5] K. Kuyanov-Prozument and A.F. Vilesov, Phys. Rev. Lett. **101**, 205301 (2008).

[6] P. Sindzingre, D.M. Ceperley and M.L. Klein, Phys. Rev. Lett. **67**, 1871 (1991).

[7] S. Grebenev, B.Sartakov, J.P.Toennies and A.F. Vilesov, Science **289**, 1532 (2000).

[8] H.Li, R.J. Le Roy, P.-N. Roy and A.R.W. McKellar, Phys. Rev. Lett. **105**, 133401 (2010).

[9] T. Zeng and P.-N. Roy, Rep. Prog. Phys. **77**, 46601 (2014).

[10] O.N. Osychenko, R. Rota and J. Boronat, Phys. Rev. B **85**, 224513 (2012).

[11] J.Turnbull and M.Boninsegni, Phys. Rev. B **78**, 144509 (2008).

[12] G. M. Zassenhaus and J. D. Reppy, Phys. Rev. Lett. **83**, 4800 (1999).

[13] R. Toda, M. Hieda, T. Matsushita, N. Wada, J. Taniguchi, H. Ikegami, S. Inagaki and Y. Fukushima, Phys. Rev. Lett. **99**, 255301 (2007).

[14] J. Yoon, D. Sergatskov, J. Ma, N. Mulders, and M.H.W. Chan, Phys. Rev. Lett. **80**, 1461 (1998).

[15] J. Nyeki, R. Ray, B.Cowan and J. Saunders, Phys. Rev. Lett. **81**, 152 (1998), and references therein.

[16] M.C. Gordillo, J. Boronat and J. Casulleras, Phys. Rev. Lett. **85**, 2348 (2000).

[17] M. Boninsegni, Phys. Rev. Lett. **111**, 235303 (2013).

[18] M. Boninsegni, Phys. Rev. B **70**, 193411 (2004).

[19] T. Omiyinka and M.Boninsegni, Phys. Rev. B **90**, 064511 (2014).

[20] A. Sarsa, K.E. Schmidt and W.R. Magro, J. Chem. Phys. **113**, 1366 (2000).

[21] M. Rossi, M. Nava, L. Reatto and D.E. Galli, J. Chem. Phys. **131**, 154108 (2009).

[22] S. Vitiello, K. Runge and M.H. Kalos, Phys. Rev. Lett. **60**, 1970 (1988).

[23] D.E. Galli and L. Reatto, Mol. Phys. **101**, 1697 (2003).

[24] M. Rossi, L. Reatto and D.E. Galli, J. Low Temp. Phys. **168**, 235 (2012).

[25] M. Rossi, E. Vitali, L. Reatto and D.E. Galli, Phys. Rev. B **85**, 014525 (2012).

[26] E. Vitali, M. Rossi, F. Tramonto, D.E. Galli and L. Reatto, Phys. Rev. B **77**, 180505R (2008).

[27] F. Operetto and F. Pederiva, Phys. Rev. B **69**, 024203 (2004).

[28] I.S. Silvera and V.V. Goldman, J. Chem. Phys. **69**, 4209 (1978).

[29] D.Y. Sun, J.W. Liu, X.G. Gong and Z-F. Liu, Phys. Rev. B **75**, 075424 (2007).

[30] See Supplemental Material at ... for details on the pH_2-CNT interaction potential V, the curvature effects and the more details on the possible experimental setup.

[31] M. Rossi, D.E. Galli and L. Reatto, Phys. Rev. B **72**, 064516 (2005).

[32] M. Rossi, D.E. Galli and L. Reatto, J. Low Temp. Phys. **146**, 95 (2007).

[33] A. Del Maestro, M. Boninsegni and I. Affleck, Phys. Rev. Lett. **106**, 105303 (2011).

[34] A. Del Maestro, Int. J. Mod. Phys. B **26**, 1244002 (2012).

[35] B. Kulchytskyy, G. Gervais and A. Del Maestro, Phys. Rev. B **88**, 064512 (2013).

[36] L. Pollet and A.B. Kuklov, Phys. Rev. Lett. **113**, 045301 (2014).

[37] L.W. Bruch, M.W. Cole and E. Zaremba, *Physical Adsorption: Forces and Phenomena* (Oxford University Press, Oxford, 1997).

[38] S. Zhang, N. Kawashima, J. Carlson and J.E. Gubernatis, Phys. Rev. Lett. **74**, 1500 (1995).

[39] M. Nava, D.E. Galli, M.W. Cole and L. Reatto, Phys. Rev. B **86**, 174509 (2012).

[40] M. Boninsegni, Phys. Rev. B **93**, 054507 (2016).

[41] C. Cazorla and J. Boronat, Phys. Rev. B **88**, 224501 (2013).

[42] M. Rossi, E. Vitali, D.E. Galli and L. Reatto, J. Phys.: Condens. Matter **22**, 145401 (2010)

[43] S.-I. Tomonaga, Prog. Theor. Phys. **5**, 544 (1950).

[44] J.M. Luttinger, J. Math. Phys. **4**, 1154 (1963).

[45] F.D.M. Haldane, Phys. Rev. Lett. **47**, 1840 (1981).

[46] T. Giamarchi, *Quantum Physics in One Dimension* (Oxford University Press, New York, 2003).

[47] Two predominant definitions of the Luttinger parameter K_L exist in the literature. The one used here is the inverse of the one employed in Ref. [17, 33–35].

[48] A. Del Maestro and I. Affleck, Phys. Rev. B. **82**, 060515R (2010).

[49] G.E. Astrakharchik and J. Boronat Phys. Rev. B **90**, 235439 (2014).

[50] G. Bertaina, M. Motta, M. Rossi, E. Vitali and D. E. Galli, Phys. Rev. Lett. **116**, 135302 (2016).

[51] N.D. Mermin and H. Wagner, Phys. Rev. Lett. **17**, 1133 (1966).

[52] T. Eggel, M.A. Cazalilla and M.Oshikawa, Phys. Rev. Lett. **107**, 275302 (2011).

[53] M.A. Cazalilla, R. Citro, T. Giamarchi, E. Orignac and M. Rigol, Rev. Mod. Phys. **83**, 1405 (2011).

[54] T. Giamarchi and H.J. Schulz, Europhys. Lett. **3**, 1287 (1987); Phys. Rev. B **37**, 325 (1988).

[55] We have fit our v_{1D} with the formula $v_{LJ}(z) = 4\varepsilon\left[\left(\frac{\sigma}{z}\right)^m - \left(\frac{\sigma}{z}\right)^{m/2}\right]$ obtaining $\varepsilon = 8.485$ K, $\sigma = 2.726$ Å and $m = 9.230$ for the (10,10) CNT and $\varepsilon = 3.683$ K, $\sigma = 2.658$ Å and $m = 8.957$ for the (15,15) one.

[56] The external potential experienced by the pH_2 molecules in the central column is the sum of the potential due to the CNT itself and the one due to the adsorbed layer. The CNT produces a periodic potential whose maximum excursion in energy (i.e. the energy difference between top and hollow site adsorption energies) are of the order of 0.03 K, i.e. 10^{-3} times the SG well and 4×10^{-3} times the v_{1D} well. The adsorbed layer produces a potential which is disordered due to the presence of defects induced by incommensurability, whose maximum excursion in energy in 0.3 K, i.e. 10^{-2} times the SG well and 4×10^{-2} times the v_{1D} well.

[57] T. Omiyinka and M.Boninsegni, Phys. Rev. B **93**, 104501 (2016).

SUPPLEMENTAL MATERIAL: SUPERFLUID BEHAVIOR OF QUASI-1D P-H_2 INSIDE CARBON NANOTUBE

PH_2-CNT INTERACTION POTENTIAL

The effective pH_2-CNT interaction potential V is constructed by summing all the pairwise pH_2-C contributions among the pH_2 molecule and the Carbon atoms of an armchair CNT tube of indices (n,n) and stored on a grid for computational efficiency. To prevent spurious boundary effects due to the truncation of the tube (and on the imposed periodic boundary conditions along the axis) we construct tubes longer than 100 Å to perform the summation but retain only the central portion of length $L_0 = 14.77$ Å (corresponding to 5 elemental cells of the Carbon hexagonal lattice). Thus the simulated CNTs described in the paper will have lengths that are integer multiples of L_0.

Curvature effects.

In order to describe the pH_2-C interaction we have considered an exp-6-8-10 potential obtained by fitting high-quality *ab initio* results for the H_2-graphite interaction [1]. Although our potential construction accounts for the cylindrical geometry of the C atoms, it misses the curvature related $sp^2 \rightarrow sp^3$ hybridization of the Carbon bonds that may modify the pH_2-C interaction. Curvature-dependent corrections to the coefficients of a Lenard-Jones potential describing the C-H_2 pairwise interaction have been proposed in the past to include effects due to the increasing $sp^2 \rightarrow sp^3$ hybridization in Carbon nanotubes as the CNT radius decreases[2]. Such corrections are based on interpolation formulas between the two extreme limits of pH_2 interacting with a C atom in a graphite plane (pure sp^2 character) and in an ideal sp^3 environment. However, this model potential was later found inadequate to quantitatively describe the H_2-graphite interaction and thus a better, albeit curvature independent, C-H_2 pair potential has been proposed [1], which we are using here. Corrections due to mixed hybridization effects mentioned above (which are important for CNTs with very small radii) are expected however to have small impact for the CNT investigated in our work. In fact, for the radii of interest here, the sp^2 component in the interaction parameter predicted by the interpolation formulas of Ref. [2] would be dominant (being 86% for the (10,10) tube and 91% for the (15,15) one). We should also add that among physisorbed system, Carbon materials represent rather attractive substrates for pH_2

adsorption, and thus relatively small changes in the adsorption well depth/position of the pH_2-C potential are expected to affect only slightly the structure of the solid-like pH_2 layer adsorbed on the CNT inner wall, and have even smaller effects on the central column structure.

In order to check that curvature effects are indeed negligible in the present study, we proceeded as in Ref. [2] to compute the interaction between H_2 and an sp^3-coordinated Carbon atom with a dangling bond, and then use their interpolation formulas to find the correction to the pair potential well-depth used in our calculation (appropriate for a flat, sp^2 coordinated substrate). We performed state-of-the-art *ab initio* calculations (using the QUANTUM-ESPRESSO package[3]) to compute the interaction between a H_2 molecule and a t-butyl radical (used in Ref. [2] to model the environment of an unsaturated sp^3 carbon). The exchange-correlation functional used in our calculations explicitly includes the contribution of dispersion (Van der Waals) forces [4] (which were neglected in the calculations of Ref. [2]), which are known to provide important corrections to the energetics of physisorbed systems like the one considered here. We find that in order to reproduce the ab-initio results described above for the H_2-C(sp^3) interaction, the well depth of the exp-6-8-10 pair potential should be $\epsilon = 6.2\,meV$, to be compared to the value $\epsilon = 5.3\,meV$ describing the pH_2-C(sp^2) two-body interaction. By using the above values in the interpolation formula that gives the curvature-corrected well depth parameter of the two-body interaction appropriate for a CNT with a given radius[2], we find that in the case of the (10,10) tube, the pair-potential well depth should be decreased by 23% with respect to the value (appropriate for the H_2-C(sp^2) interaction) used in our calculations. An even smaller change is found for the (15,15) tube. In order to estimated the consequences of such a reduction, we compare the results of the QMC calculations for the radial density profile in the (10,10) CNT by summing (i) the pair potential without curvature corrections V (i.e. the one used for the computation in the main paper) and (ii) a rescaled one ηV with $\eta = 0.9$, 0.8 and 0.7. We find, as it appears in Fig. 4 where our results are reported, that the differences in the two cases (i.e. with and without curvature corrections) are indeed very small. The maximum of the density peak is reduced by a factor about 9% for the largest considered η, but even in this case the number of pH_2 molecules housed by the adsorbed layer is the same as for $\eta = 1.0$. Since the curvature effects on the density profiles are small, the obtained effective one-dimensional interaction potential v_{1D} (Eq.(3) in the main paper) is practically insensitive to such corrections, as can be inferred from the right panel of Fig. 4. This confirms that curvature effects are completely negligible for the present study.

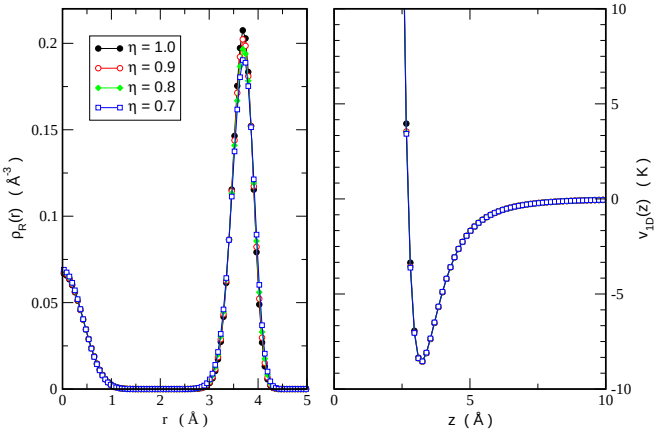

FIG. 4: (Color online) Left panel: radial density profiles $\rho_R(r)$ for pH_2 inside a (10,10) CNTs with the potential V rescaled by a factor η as described in the text. Statistical errors are smaller than the used symbols. Right panel: corresponding effective one-dimensional interaction potential v_{1D}.

POSSIBLE EXPERIMENTAL SETUP TO OBSERVE PH_2 SUPERFLUID BEHAVIOR IN CNTS.

Aligned structures of CNTs (of lengths up to hundreds microns) with controllable radii can be routinely grown on different substrates (see for instances Ref. [5], and references therein). Micrometer-sized bundles of aligned parallel carbon nanotubes have been grown, in particular, on silicon or quartz surfaces [6], which can be up to 300 micron tall, with a bundle aspect ratio (height-to-width) of 5:1. This is a particularly favorable method in the present context, which allow in principle to grow the CNTs bundle directly over a quartz crystal microbalance (QCM) surface. Once filled with hydrogen (whose amount can be controlled through the environmental pressure), frequency shifts in the shear modes of the microbalance parallel to the bundle axis should allow detection of mass decoupling due to the appearance (e.g. by lowering the temperature) of a superfluid fraction within the central column of pH_2 in each CNT. The latter corresponds to about 3% of the total amount of pH_2 adsorbed in a (10,10) CNT. For a QCM driven at a fundamental frequency of 5 MHz, adsorption of pH_2 in the nanotubes will determine a frequency shift of 30 Hz if the total open volume of the nanotubes amounts to, say, $10^{-7}\,cc$ (which is well below the theoretical values accessible in the microscopic bundles described above). If about 3% of the total pH_2 mass decouples from the QCM oscillations in the superfluid phase, this will determine an increase in the resonance frequency of about 1 Hz, which is well above the standard resolution of 0.1 Hz (or less) typical of a QCM setup (see, for instance, Ref. [7]), thus allowing, in principle, to detect the normal-to-superfluid transition.

[1] D.Y. Sun, J.W. Liu, X.G. Gong and Z-F. Liu, Phys. Rev. B **75**, 075424 (2007).
[2] M. K. Kostov, H. Cheng, A.C. Cooper and G.P. Pez, Phys. Rev. Lett. **89**, 146105 (2002).
[3] P. Giannozzi, S. Baroni, N. Bonini, M. Calandra, R. Car, C. Cavazzoni, D. Ceresoli, G.L. Chiarotti, M. Cococcioni, I. Dabo, A. Dal Corso, S. de Gironcoli, S. Fabris, G. Fratesi, R. Gebauer, U. Gerstmann, C. Gougoussis, A. Kokalj, M. Lazzeri, L. Martin-Samos, N. Marzari, F. Mauri, R. Mazzarello, S. Paolini, A. Pasquarello, L. Paulatto, C. Sbraccia, S. Scandolo, G. Sclauzero, A.P. Seitsonen, A. Smogunov, P. Umari and R.M. Wentzcovitch, J. Phys.: Condens. Matter **21**, 395502 (2009).
[4] K. Lee, E.D. Murray, L. Kong, B.I. Lundqvist and D.C. Langreth, Phys. Rev. B **82**, 081101(R) (2010).
[5] G. Chen, Scientific Reports **4**, 3804 (2014).
[6] Technical report of the U.S. patent US 20010019238.
[7] L. Bruschi and G. Mistura, Phys. Rev. B. **63**, 235411 (2001).